Heat Mass Transfer (2009) 45:1473–1482
DOI 10.1007/s00231-009-0525-6

ORIGINAL

Thermophoretic deposition of particles in fully developed mixed convection flow in a parallel-plate vertical channel: the full analytical solution

Eugen Magyari

Received: 11 November 2008 / Accepted: 2 August 2009 / Published online: 15 August 2009

Abstract In a recent paper (Grosan et al. in Heat Mass Transf 45:503–509, 2009) a mostly numerical approach to the title problem has been reported. In the present paper the full analytical solution is given. Several new features emerging from this approach are discussed in detail.

1 Introduction

Thermophoresis is the phenomenon by which submicron sized particles (as soot particles, aerosols, etc.) suspended in a nonisothermal gas migrate in the direction of decreasing temperature with a velocity which is proportional to the local temperature gradient. According to this basic feature, thermophoresis is a widely spread phenomenon in nature and technical processes, causing both desirable effects (e.g., cleaning of gas streams in thermal precipitators, enhanced mass transfer in the modified chemical vapor deposition processes, etc.), as well as undesirable ones (staining of surfaces of heat exchangers, dirt patterns on the facades of buildings, on the ceilings of kitchens and dining rooms, etc.).

The fundamental physical processes responsible for the thermophoresis were investigated already in the nineteenth century by Maxwell. Since then, on this phenomenon and its applications a vast and widely ramified literature has been accumulated. Concerning the thermophoretic transport involved in viscous flow and in flow in porous media for various geometries and boundary conditions, a comprehensive review of the pertinent literature has recently been given by Grosan et al. [1], Selim et al. [2], Postelnicu [3] and Chamkha and Pop [4]. As emphasized in [2], the first studies in this respect were conducted on simple one-dimensional flows. In a laser-Doppler velocimeter study of velocity profiles in the laminar boundary layer adjacent to a heated flat plate, Talbot et al. [5] have shown that the seed particles used for the measurements were driven away from the plate surface by thermophoretic forces, causing a particle-free region within the boundary layer of approximately one half the boundary-layer thickness. It has been evidenced that the theory of Brock [6], with an improved value for the thermal slip coefficient, gives the best agreement with experiment for low Knudsen numbers. The first analysis of thermophoretic deposition in a geometry of engineering interest appears to be that of Hales et al. [7]. They solved the laminar boundary layer equations for simultaneous aerosol and steam transport to an isothermal vertical surface. Thermophoresis in laminar flow over a horizontal flat plate for both cold and hot surface conditions has been studied theoretically by Goren [8]. In the paper of Epstein et al. [9], the thermophoretic transport of small particles through a free convection boundary layer adjacent to a cold, vertical deposition surface was analyzed. Considerations concerning the rate of thermophoretic deposition which is as general as possible in its application to different flow fields were presented by Batchelor and Shen [10]. The thermophoretic deposition of the laminar slot jet on an inclined plate for hot, cold and adiabatic surface conditions with viscous dissipation effect was examined by Garg and Jayaraj [11]. The thermophoretic transport of aerosol particles through a forced convection laminar boundary layer in cross flow over a cylinder for hot, cold and adiabatic wall conditions has also been investigated by Garg and Jayaraj [12]. More recently, Chein and Liao [13] have presented a numerical model

E. Magyari (✉)
Institut für Hochbautechnik, ETH Zürich, Wolfgang-Pauli Str.1, 8093 Zurich, Switzerland
e-mail: magyari@hbt.arch.ethz.ch; magyari@bluewin.ch

including both the particle molecular diffusion and thermophoretic effects to study nanoparticle deposition in a 2D channel flow. The combined effect of inertia, diffusion and thermophoresis on particle deposition from a stagnation point flow onto an axisymmetric wavy wafer, has been examined by Wang [14]. A mathematical model for the coupled transport mechanisms of diffusion, convection and thermophoresis was developed by Wang and Chen [15] to describe the particle deposition onto a continuous moving wavy surface.

The present paper is closely related to a recent article of Grosan et al. [1] in which a study of thermophoretic transport in the steady fully developed mixed convection flow in a parallel-plate vertical channel with differentially heated isothermal walls has been presented. In this case the temperature distribution between the walls is described by a simple linear function of the transverse coordinate, such that the main task of the paper [1] was the solution of the pertinent boundary value problems for the concentration and velocity fields. These (simply coupled) two-point boundary value problems were solved in [1] numerically by using finite differences. However, bearing in mind that the governing dimensionless differential equations of the concentration and velocity fields involve, in addition to the unknown pressure gradient α, further six dimensionless parameters (N_t, N_c, λ, B, k and Sc, [1]) a comprehensive numerical study of the basic velocity, concentration and pressure characteristics is extremely laborious. This parametric-complexity gave the motivation for the present paper, to report the full analytical solution of the problem examined numerically in [1]. The main benefit resulting from the analytical approach is a transparent dependence of the quantities of engineering interest on the governing parameters. Several new features emerging from this approach will be discussed in detail.

2 Governing equations

Following Grosan et al. [1], we consider the steady mixed convection flow of a gas containing suspended aerosol particles in a vertical parallel plane channel of width L. The walls at $x = 0$ and $x = L$ are kept at the constant temperatures T_h (hot wall) and $T_c < T_h$ (cold wall) as well as at the uniform concentrations C_h and C_c, respectively. It is assumed that, in addition to the pressure forces, the buoyancy forces are significant and that the Boussinesq approximation holds. In the fully developed regime the velocity, temperature and concentration fields (u, 0, 0), T and C depend only on the transverse coordinate y and are governed by the equations [1]

$$\mu\frac{d^2u}{dy^2}+\rho_0 g\left[\beta_T(T-T_0)+\beta_C(C-C_0)\right]-\frac{\partial p}{\partial x}=0 \tag{1}$$

$$\frac{d^2T}{dy^2}=0 \tag{2}$$

$$D\frac{d^2C}{dy^2}=\frac{d}{dy}(v_TC) \tag{3}$$

subject to the boundary conditions

$$\begin{aligned} &u(0)=0, \quad T(0)=T_h, \quad C(0)=C_h,\\ &u(L)=0, \quad T(L)=T_c, \quad C(L)=C_c \end{aligned} \tag{4}$$

The thermophoretic deposition velocity v_T is related to the temperature field by the well known relationship

$$v_T=-k\frac{\mu}{\rho_0 T}\frac{dT}{dy} \tag{5}$$

and in Eq. 1 the reference temperature T_0 and the reference concentration C_0 of the Boussinesq approximation have been chosen equal to the average values of the corresponding wall quantities, $T_0=(T_h+T_c)/2$ and $C_0=(C_h+C_c)/2$, respectively. Furthermore (in the fully developed flow regime) the gradient $\partial p/\partial x$ of the hydrodynamic pressure is a constant quantity and thus, besides the six integration constants occurring in the solutions of Eqs. 1–3, it represents the seventh unknown constant of the problem. On this reason, in addition to the six boundary conditions (4) a further condition is necessary in order to have a mathematically well-posed problem. With this aim, in the mixed convection duct flow problems it is usual to prescribe also the value of the volumetric flow rate in a transversal section of the channel

$$Q=\int_0^L u\,dy \tag{6}$$

which in flow experiments is a directly accessible quantity.

Introducing the dimensionless quantities [1]

$$\begin{aligned} &Y=\frac{y}{L}, \quad U=\frac{u}{U_0}, \quad U_0=\frac{Q}{L}, \quad \theta=\frac{T-T_0}{T_h-T_c},\\ &\phi=\frac{C-C_0}{C_h-C_c}, \quad \alpha=\frac{L}{\mu U_0}\frac{\partial p}{\partial x},\\ &Gr=\frac{g\beta_T(T_h-T_c)L^3}{(\mu/\rho_0)^2}, \quad Re=\frac{U_0L}{(\mu/\rho_0)}, \quad \lambda=\frac{Gr}{Re},\\ &b=\frac{\beta_c(C_h-C_c)}{\beta_T(T_h-T_c)},\\ &N_t=\frac{1}{2}\frac{T_h+T_c}{T_h-T_c}, \quad N_c=\frac{1}{2}\frac{C_h+C_c}{C_h-C_c}, \quad Sc=\frac{\mu}{\rho_0 D} \end{aligned} \tag{7}$$

the boundary value problem (1)–(6) goes over in the form [1]

$$\frac{d^2U}{dY^2} + \lambda(\theta + b\phi) - \alpha = 0 \tag{8}$$

$$\frac{d^2\theta}{dY^2} = 0 \tag{9}$$

$$\frac{d^2\phi}{dY^2} = -kSc\frac{d}{dY}\left(\frac{N_c + \phi}{N_t + \theta}\frac{d\theta}{dY}\right) \tag{10}$$

$$\begin{aligned} U(0) &= 0, \quad \theta(0) = \phi(0) = \frac{1}{2}, \\ U(1) &= 0, \quad \theta(1) = \phi(1) = -\frac{1}{2} \end{aligned} \tag{11}$$

$$\int_0^1 U dY = 1 \tag{12}$$

In the above equations, everywhere the notations of [1] have been used, except for the buoyancy ratio b which in [1] has been denoted by B.

3 The analytical solution

The solution for the dimensionless temperature θ is immediate, [1],

$$\theta = \frac{1}{2} - Y \tag{13}$$

Now, it is seen that the key problem consists of the solution of the ϕ Eq. 10 since (in addition to θ), ϕ is involved in the velocity Eq. 8 explicitly. In the numerical approach reported in [1], the full second order Eq. 10, with θ given by Eq. 13, has been solved numerically for different values of the parameters involved. The present analytical approach avoids this way by noticing that Eq. 10 admits the first integral

$$\frac{d\phi}{dY} = -kSc\frac{N_c + \phi}{N_t + \theta}\frac{d\theta}{dY} + K_1 = kSc\frac{N_c + \phi}{\left(N_t + \frac{1}{2}\right) - Y} + K_1 \tag{14}$$

where K_1 is a constant of integration. Introducing the new independent variable Z as well as the notation a specified by equations

$$Z = \left(N_t + \frac{1}{2}\right) - Y, \quad a = kSc \tag{15}$$

Equation 14 becomes

$$\frac{d\phi}{dZ} = -\frac{a(N_c + \phi)}{Z} - K_1 \tag{16}$$

It is worth noticing here that $a = kSc$ is not only a convenient short notation, but it emphasizes the physically important feature that the boundary value problem (8)–(12) does not depend on the (dimensionless) thermophoretic coefficient k and the Schmidt number Sc separately, but on their product kSc only. In other words, the concentration distributions ϕ of the fully developed channel flow associated with different values of k and Sc, but with the same value of the *effective thermophoretic coefficient* $a = kSc$ (as well as of N_t and N_c), are physically equivalent. Obviously, this *principle of equivalent states* is a consequence of the interplay between thermophoresis (driven by temperature gradients) and diffusion (driven by concentration gradients).

Fortunately, Eq. 16 can be integrated once more, yielding the explicit analytical solution

$$\phi = -N_c - \frac{K_1}{1 + a}Z + \frac{K_2}{Z^a} \tag{17}$$

where K_2 is the second constant of integration of Eq. 10. Bearing in mind the ϕ boundary conditions (11), we obtain for the constants K_1 and K_2 the expressions

$$\begin{aligned} K_1 &= \frac{1 + a}{2}\frac{(2N_c + 1)Z_0^a - (2N_c - 1)Z_1^a}{Z_1^{1+a} - Z_0^{1+a}}, \\ K_2 &= \frac{(N_t - N_c)(Z_0Z_1)^a}{Z_1^{1+a} - Z_0^{1+a}} \end{aligned} \tag{18}$$

where

$$\begin{aligned} Z_0 &\equiv \phi|_{Y=0} = N_t + \frac{1}{2} = \frac{T_h}{T_h - T_c}, \\ Z_1 &\equiv \phi|_{Y=1} = N_t - \frac{1}{2} = \frac{T_c}{T_h - T_c} \end{aligned} \tag{19}$$

Thus, the explicit expressions for K_1 and K_2 in terms of N_t, N_c and a are

$$\begin{aligned} K_1 &= -(1 + a)\frac{(2N_c + 1)(2N_t + 1)^a - (2N_c - 1)(2N_t - 1)^a}{(2N_t + 1)^{1+a} - (2N_t - 1)^{1+a}}, \\ K_2 &= -\frac{2^{1-a}(N_t - N_c)\left(4N_t^2 - 1\right)^a}{(2N_t + 1)^{1+a} - (2N_t - 1)^{1+a}} \end{aligned} \tag{20}$$

Accordingly,

$$\begin{aligned} \phi = -N_c &+ \frac{(2N_c + 1)(2N_t + 1)^a - (2N_c - 1)(2N_t - 1)^a}{(2N_t + 1)^{1+a} - (2N_t - 1)^{1+a}}Z \\ &- \frac{2^{1-a}(N_t - N_c)\left(4N_t^2 - 1\right)^a}{(2N_t + 1)^{1+a} - (2N_t - 1)^{1+a}}\frac{1}{Z^a} \end{aligned} \tag{21}$$

In this way, the analytical solution of the ϕ-problem is also available in an explicit form. Notice that, in view of the respective Eq. 7, for the allowed values of N_t and N_c the inequalities $N_t > 1/2$ and $N_c > 1/2$ hold. Thus, in Eqs. 20 and 21, no singularities and no imaginary quantities can occur.

Let us now turn to the velocity problem. Substituting Eqs. 13, 15 and 17 in Eq. 10, we obtain

$$\frac{d^2U}{dZ^2} = \alpha + \lambda(N_t + bN_c) - \lambda\left(1 - \frac{bK_1}{1 + a}\right)Z - \frac{\lambda bK_2}{Z^a} \tag{22}$$

Two subsequent integrations of Eq. 22 lead for the dimensionless velocity to the explicit solution

$$U = K_4 + K_3 Z + \frac{1}{2}[\alpha + \lambda(N_t + bN_c)]Z^2 - \frac{\lambda}{6}\left(1 - \frac{bK_1}{1+a}\right)Z^3 - \frac{\lambda bK_2}{(1-a)(2-a)}Z^{2-a} \quad (23)$$

where K_3 and K_4 are the two constants of integration of Eq. 22, for which the U-boundary conditions give the relationships

$$K_3 = -\frac{1}{2}[\alpha + \lambda(N_t + bN_c)]\left(Z_0^2 - Z_1^2\right) + \frac{\lambda}{6}\left(1 - \frac{bK_1}{1+a}\right) \times \left(Z_0^3 - Z_1^3\right) + \frac{\lambda bK_2}{(1-a)(2-a)}\left(Z_0^{2-a} - Z_1^{2-a}\right),$$

$$K_4 = -\frac{1}{2}[\alpha + \lambda(N_t + bN_c)]\left(Z_0 Z_1^2 - Z_1 Z_0^2\right) + \frac{\lambda}{6}\left(1 - \frac{bK_1}{1+a}\right)\left(Z_0 Z_1^3 - Z_1 Z_0^3\right) + \frac{\lambda bK_2}{(1-a)(2-a)}\left(Z_0 Z_1^{2-a} - Z_1 Z_0^{2-a}\right) \quad (24)$$

Furthermore, the integral condition Eq. 12 yields

$$1 = -\int_{Z_0}^{Z_1} U dZ = K_4(Z_0 - Z_1) + \frac{1}{2}K_3\left(Z_0^2 - Z_1^2\right) + \frac{1}{6}[\alpha + \lambda(N_t + bN_c)]\left(Z_0^3 - Z_1^3\right) - \frac{\lambda}{24}\left(1 - \frac{bK_1}{1+a}\right) \times \left(Z_0^4 - Z_1^4\right) - \frac{\lambda bK_2}{(1-a)(2-a)(3-a)}\left(Z_0^{3-a} - Z_1^{3-a}\right) \quad (25)$$

The explicit solution of Eq. 25 with respect to the dimensionless pressure gradient α is

$$\alpha = -12 + \frac{3\lambda b(N_t - N_c)\left(4N_t^2 - 1\right)^a}{(2N_t+1)^{1+a} - (2N_t-1)^{1+a}} \times \left[\frac{(2N_t+1)^a + (2N_t-1)^a}{3\left(4N_t^2-1\right)^a} + \frac{(2N_t + a - 2)(2N_t+1)^{2-a} - (2N_t - a + 2)(2N_t-1)^{2-a}}{(1-a)(2-a)(3-a)}\right] \quad (26)$$

4 Discussion

Equations 13, 21, 23 and 26 give the explicit analytical solutions of the title problem for the dimensionless temperature θ, concentration ϕ velocity U and pressure gradient α, respectively. The aim of the present section is to discuss some basic features of these solutions.

4.1 The temperature field

The linear temperature distribution (13) between the isothermal walls of the channel is a simple textbook issue and does not require any additional comment.

4.2 The concentration field

Concerning the expression (21) of the concentration field ϕ, we first notice that it depends on the transformed transverse coordinate Z (specified by Eq. 15) in a pure algebraic way, including in addition to the linear term in Z also a strongly nonlinear term proportional to $1/Z^a$. It is also worth emphasizing here explicitly, that ϕ depends neither on the mixed convection parameter λ, nor on the buoyancy ratio b. Its explicit expression (21) involves only the parameters N_t, N_c and $a = kSc$.

Bearing in mind the first integral (14) of the concentration Eq. 10 as well as the boundary conditions (11), the values of Sherwood number (i.e., of the negative concentration gradients at the walls of the channel)

$$Sh_{0,1} = -\left.\frac{d\phi}{dY}\right|_{Y=0,1} \quad (27)$$

can also be calculated easily. The result is.

$$Sh_0 = -a\frac{2N_c+1}{2N_t+1} + (1+a)\frac{(2N_c+1)(2N_t+1)^a - (2N_c-1)(2N_t-1)^a}{(2N_t+1)^{1+a} - (2N_t-1)^{1+a}},$$

$$Sh_1 = -a\frac{2N_c-1}{2N_t-1} + (1+a)\frac{(2N_c+1)(2N_t+1)^a - (2N_c-1)(2N_t-1)^a}{(2N_t+1)^{1+a} - (2N_t-1)^{1+a}} \quad (28)$$

The two Sherwood numbers are related to each other by the relationship

$$Sh_1 = Sh_0 + 4a\frac{N_t - N_c}{4N_t^2 - 1} \quad (29)$$

The second term on the right hand side of Eq. 29 represents the thermophoretic deposition flux of the particles on the cold wall when $N_t > N_c$ and the ablation flux from the same wall when $N_t < N_c$. We mention that, with respect to the wall conditions, the inequality $N_t > N_c$ corresponds to the situation in which $T_c/T_h > C_c/C_h$ and $N_t < N_c$ to $T_c/T_h < C_c/C_h$, respectively. It is also interesting to notice that for $N_t = N_c$ and arbitrary a on the one hand, and for $a = 0$ and arbitrary N_t and N_c on the other hand, the Sherwood numbers render same value $Sh_0 = Sh_1 = 1$.

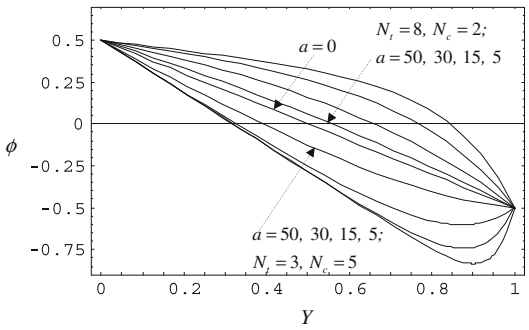

Fig. 1 Plots of the dimensionless concentration profiles ϕ for the indicated values of the parameters a, N_t and N_c

Beyond this somewhat surprising feature stands the fact that, according to Eq. 21, in both of these cases the same relationship holds.

$$\phi = \frac{1}{2} - Y = \theta \tag{30}$$

As an illustration, in Fig. 1 the dimensionless concentration profiles ϕ are plotted for the indicated values of the parameters $a = kSc$, N_t and N_c. The four upper curves correspond to a case with $N_t > N_c$ and descend monotonically from the left to the right wall of the channel, changing sign somewhere in the range $1/2 < Y < 1$. The four lower curves correspond to an opposite case, $N_t < N_c$. The two families of curves reduce for $a = 0$ to the same straight line which represents Eq. 30. The lower curves change sign somewhere in the range $0 < Y < 1/2$, and then descend monotonically either to the right-wall value $\phi = -1/2$, or to a minimum value $\phi_{\min} < -1/2$ reached at some $Y = Y_*$. In the latter case the concentration curves ascend then from the minimum to the wall value $\phi = -1/2$ as $Y \to 1$. It can be shown that

$$Y_* = N_t + \frac{1}{2} - \left[-a(1+a)\frac{K_2}{K_1}\right]^{\frac{1}{1+a}},$$
$$\phi_{\min} = -N_c - \frac{K_1}{1+a}\left[-a(1+a)\frac{K_2}{K_1}\right]^{\frac{1}{1+a}} + K_2\left[-a(1+a)\frac{K_2}{K_1}\right]^{\frac{-a}{1+a}} \tag{31}$$

The necessary and sufficient conditions for existence of the minimum (31) are

$$N_t < N_c,$$
$$\frac{2N_c - 1}{2N_c + 1}\left[\left(\frac{2N_t - 1}{2N_t + 1}\right)^a + \frac{4a(N_c - N_t)}{(2N_t - 1)(2N_c - 1)}\right] > 1 \tag{32}$$

4.3 The velocity field

Let us now turn to the more complex problem of the velocity field U, described by the explicit analytical solution (23). In general, the velocity U depends via K_1, K_2; K_3, K_4 and α, given by Eqs. 20, 24 and Eq. 26, on all five dimensionless parameters N_t, N_c, a, b and λ of the problem. We start the discussion of this intricate dependence with four special cases, which are:

(i) $\lambda = 0$, whereas N_t, N_c, a and b are arbitrary,
(ii) $b = 0$, whereas N_t, N_c, a and λ are arbitrary,
(iii) $a = 0$, whereas N_t, N_c, b and λ are arbitrary,
(iv) $N_t = N_c$, whereas a, b and λ are arbitrary.

All these four cases share the property that the dimensionless pressure gradient α takes the same constant value

$$\alpha = -12 \quad (\text{in all cases(i)} - \text{(iv)}) \tag{33}$$

Case (i) corresponds to the forced convection flow. Accordingly, in Eq. 23 one recovers the classical Poiseuille law $U = 6Y(1 - Y)$ for the plane-parallel channel flow. The concentration field ϕ due to mass diffusion and thermophoresis is independent of λ and b, and thus it coexists in its general form (21) with the velocity field $U = 6Y(1 - Y)$ of the Poiseuille flow.

Case (ii) occurs when the buoyancy effect related to the concentration gradients is negligible compared to the thermal buoyancy, i.e., when in Eq. 1 the relationship $|\beta_C\,(C - C_0)| \ll |\beta_T\,(T - T_0)|$ holds. This physical situation corresponds in the basic dimensionless Eqs. 8–12 to the limiting case $b \to 0$ (while $C_t \neq C_c$). In this limiting case of the vanishing buoyancy ratio, the explicit solutions (13) and (21) for θ and ϕ remain unchanged, and Eqs. 23 and 24 give for the flow velocity U the result

$$U = 6Y(1 - Y)\left[1 - \frac{\lambda}{72}(2Y - 1)\right] \quad (\text{case(ii)}) \tag{34}$$

Therefore, the velocity field is independent of N_t, N_c and a when $b = 0$. This result, although at the first sight physically somewhat surprising, could have been predicted from the very beginning, since in the velocity Eq. 8 the term $b\phi$ which involves the parameters N_t, N_c and a disappears as $b \to 0$. It is also worth mentioning here that Eq. 34 is in fact equivalent to Eq. 17a of Aung [16], although in [16] no thermophoretic transport has been assumed at all.

Cases (iii) and (iv) lead to quite surprising results. As already mentioned in Sect. 4.2, in these cases for the temperature and concentration fields the same relationship (30) results, and thus the Sherwood numbers render same value $Sh_0 = Sh_1 = 1$. After some algebra we arrive to the conclusion that also for the flow velocities in both of these cases the same relationship holds, namely

$$U = 6Y(1 - Y)\left[1 - \frac{\lambda(1 + b)}{72}(2Y - 1)\right]$$
$$(\text{cases(iii) and (iv)}) \tag{35}$$

The coincidence of the velocity fields in cases (iii) and (iv) could have been predicted already by a simple

inspection of the basic Eqs. 8–12 and Eq. 30. Indeed, Eq. 10, which is the only equation containing N_t and N_c, reduces in the cases (iii) and (iv) to equation $d^2\phi/dY^2 = 0$ which does not involve N_t and N_c any more. As a consequence, in the fully developed flow regime, the case with thermophoresis $a \neq 0$ and $N_t = N_c$ on the one hand, and the case $N_t \neq N_c$ without thermophoresis, $a = 0$, on the other hand, become undistinguishable. In both of these cases, the experimentally accessible quantities θ, ϕ, U and α are the same. In other words, between the thermophoretic effect governed by the parameter a and the temperature and concentration boundary conditions governed by the parameters N_t and N_c a remarkable compensation effect can occur which renders the cases (iii) and (iv) equivalent. Moreover, for $b = 0$, Eq. 35 reduces to Eq. 34 which holds for all values of the parameters N_t, N_c, a and λ. We also mention here that in case (iii), i.e., in the absence of thermophoresis, the solution (35) has also been reported by Grosan et al. [1]. However, as we are aware, the surprising compensation effect occurring in cases (iii) and (iv) has never been reported in the literature.

A further interesting property of the velocities (34) and (35) is that in the midplane $Y = 1/2$ of the channel they take the same value, regardless the values of the parameters involved. Indeed, it is easy to show that for Eqs. 34 and 35 the relationship holds

$$U\left(\frac{1}{2}\right) = \frac{3}{2} \quad \text{(cases(iii) and (iv))}. \tag{36}$$

In addition to the features discussed above, the velocity solutions (34) and (35) possess a further interesting property which represents a general characteristic of the present channel flow (see also below). This consists of a possible crossover from a unidirectional (upward directed) flow regime to a bidirectional regime, in which in the neighborhood of the cold wall a reversed (downward directed) flow domain can occur. A simple inspection of the second Eq. 35 shows that this crossover takes place when the square bracket term becomes negative at $Y = 1$, i.e., when b exceeds the critical value b_{crit},

$$b \geq b_{\text{crit}} = \frac{72}{\lambda} - 1 \quad \text{(cases(iii) and (iv))} \tag{37}$$

Therefore, Eq. 37 specifies the necessary and sufficient condition for the occurrence of the bidirectional flow in the cases (iii) and (iv). This phenomenon is illustrated in Fig. 2. The intersection point of all the velocity profiles shown in Fig. 2 corresponds to the property (36).

We now continue to discuss further peculiarities of the exact velocity solution (23). At the first glance there seems that in addition to Z, Z^2 and Z^3, the term involving Z^{2-a} always contributes to U by a further power of Z, regardless the value of a. In general this statement is true, except for

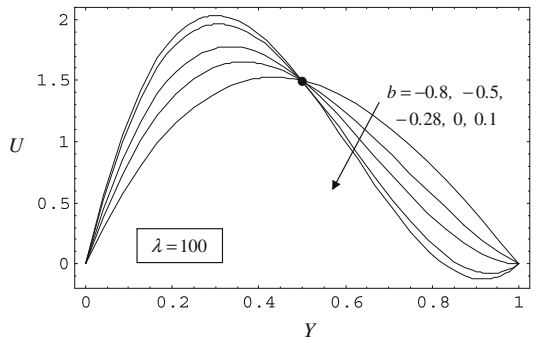

Fig. 2 Shown are the dimensionless velocity profiles (35) for $\lambda = 100$ and the indicated values of b. According to Eq. 37, the crossover from the unidirectional to the bidirectional flow regime takes place when b exceeds the critical value $b_{\text{crit}} = -0.28$ (the third curve). The intersection point of the velocity curves marked by a *dot* corresponds to the property (36)

$a = 1$ and $a = 2$, where the last term of U becomes singular. However, this is not a genuine, but an apparent singularity only, since, finally it gets compensated by the corresponding singularities occurring in the expressions (24) of K_3 and K_4, respectively. The result of this compensation is the occurrence in U of a logarithmic term of Z. This new term can be obtained by a careful calculation of limiting value of U as $a \to 1$ and $a \to 2$, respectively. An alternate way to this limiting procedure is to solve Eq. 22 from the very beginning for the special cases $a = 1$ and $a = 2$, respectively. In this way, it is immediately seen that for $a = 1$ the logarithmic term lnZ occurs already by the first integration and in the case $a = 2$ only by the second integration of Eq. 22. Obviously, both procedures lead to the same result. Thus, the velocity U and the dimensionless pressure gradient α are given in these cases as follows

Case $a = 1$:

$$\begin{aligned} U = {} & 6Y(1-Y)\left\{1 + \frac{\lambda}{72}(1-2Y)\right. \\ & + \frac{b\lambda}{144}\left[(1 - 9N_t + 36N_t^3 - 2Y)\right. \\ & \left.\left. + \frac{N_c}{N_t}(1 + 9N_t - 36N_t^3 - 2Y)\right]\right\} \\ & + \frac{b\lambda}{32}\left(1 - \frac{N_c}{N_t}\right)(4N_t^2 - 1)(2N_t - 1) \\ & \times \left[(1 + 6N_t)Y - 3(2N_t + 1)Y^2\right]\ln\left(N_t - \frac{1}{2}\right) \\ & + \frac{b\lambda}{32}\left(1 - \frac{N_c}{N_t}\right)(4N_t^2 - 1) \\ & \times \left\{(2N_t + 1)[2 + 3(2N_t - 1)Y]\right. \\ & \left. \times (Y-1)\ln\left(N_t + \frac{1}{2}\right) + 4Z\ln Z\right\} \end{aligned} \tag{38}$$

$$\alpha = -12 + \frac{\lambda b}{4}(N_t - N_c) \times \left[5 - 12N_t^2 + \frac{3}{4N_t}\left(4N_t^2 - 1\right)^2 \ln\left(\frac{2N_t + 1}{2N_t - 1}\right)\right] \quad (39)$$

Case $a = 2$:

$$U = 6Y(1-Y)\left[1 + \frac{\lambda}{72}(1-2Y)\right] + \frac{b\lambda Y(1-Y)}{12\left(1+12N_t^2\right)}\left[1 + 4N_t(N_t + 2N_c) - 18(N_t - N_c) \times \left(1 - 8N_t^2 + 16N_t^4\right) - 2\left(1 + 8N_tN_c + 4N_t^2\right)Y\right] + \frac{b\lambda(N_t - N_c)\left(1 - 4N_t^2\right)^2}{4\left(1+12N_t^2\right)}\left[(1-Y)(1+6N_tY) \times \ln\left(N_t + \frac{1}{2}\right) + (1 - 6N_t + 6N_tY)Y\ln\left(N_t - \frac{1}{2}\right) - \ln Z\right] \quad (40)$$

$$\alpha = -12 + \frac{\lambda b(N_t - N_c)}{1 + 12N_t^2}\left[4\left(1 - 5N_t^2 + 12N_t^4\right) - 3N_t\left(4N_t^2 - 1\right)^2 ln\left(\frac{2N_t + 1}{2N_t - 1}\right)\right] \quad (41)$$

One sees that the logarithmic term *lnZ* there indeed occurs in both the velocity expressions (38) and (40) explicitly.

In the general case, the existence domain of the bidirectional flow is obtained from the condition

$$\left.\frac{dU}{dY}_{Y=1}\right| \geq 0 \quad (42)$$

which requires that the slope of the velocity (23) changes at right wall of the channel $Y = 1$ from negative to positive values. After some algebra, Eq. 42 yields

$$b \geq b_{\text{crit}} = \left(\frac{72}{\lambda} - 1\right) \times \frac{(a-1)(a-2)(a-3)\left[(2N_t+1)^{1+a} - (2N_t-1)^{1+a}\right]}{(2N_t+1)^a Q_1 - (2N_t-1)^a Q_2} \quad (43)$$

where

$$Q_1 = (2N_c+1)a^3 - 6[1 + 2N_t(1 + 2N_c - 2N_t)]a^2 + \left[11 - 12N_t\left(8N_t^2 + 2N_t - 3\right) + 2N_c\left(48N_t^2 + 12N_t - 7\right)\right]a + 6(N_c - 3N_t - 1) + 36N_t(N_t - N_c)\left(4N_t^2 + 2N_t - 1\right),$$

$$Q_2 = (2N_c - 1)a^3 - 6(2N_c - 1)a^2 - \left[11 - 12N_t(2N_t+1)^2 + 2N_c\left(24N_t^2 + 24N_t - 5\right)\right]a + 6(N_c - 3N_t + 1) + 36N_t(N_t - N_c)\left(4N_t^2 + 2N_t - 1\right) \quad (44)$$

In the cases (iii) and (iv) one recovers from Eq. 43 the elementary result (37). It is important to emphasize here that the critical buoyancy ratio (43) actually does not become zero as $a \to 1$, $a \to 2$ or $a \to 3$, but approaches the limiting values

$$b_{\text{crit}} \to \left(\frac{72}{\lambda} - 1\right)\begin{cases} \frac{8N_t}{D_1} & \text{as } a \to 1 \\ \frac{1+12N_t^2}{D_2} & \text{as } a \to 2 \\ \frac{16N_t\left(1+4N_t^2\right)}{D_3} & \text{as } a \to 3 \end{cases} \quad (45)$$

where the denominators $D_{1,2,3}$ are specified as follows

$$D_1 = 8(2N_t - N_c) - 3(N_t - N_c) \times \left[4N_t\left(12N_t^2 + 4N_t - 3\right) - (2N_t+1)^2 \times \left(12N_t^2 - 8N_t + 1\right)\ln\frac{2N_t+1}{2N_t-1}\right],$$

$$D_2 = 1 - 12N_c + 4N_t\left(6N_t^2 - 1\right)\left(12N_t^2 + 2N_t - 3\right) - (6N_t+1)\left[4N_tN_c\left(12N_t^2 - 5\right) + 3(N_t - N_c) \times \left(4N_t^2 - 1\right)^2 \ln\frac{2N_t+1}{2N_t-1}\right], \quad (46)$$

$$D_3 = 16\left(N_c + 4N_t^3\right) - 3(N_t - N_c) \times \left[4N_t\left(48N_t^4 - 32N_t^2 + 5\right) - 3\left(4N_t^2 - 1\right)^3 \ln\frac{2N_t+1}{2N_t-1}\right]$$

A simple inspection of Eqs. 43 and 45 shows that $b_{\text{crit}} = 0$ when $\lambda > 72$. There also can be shown that $b_{\text{crit}} > 0$ when $\lambda > 72$ and $b_{\text{crit}} < 0$ when $\lambda > 72$, for all (positive) values of the parameters N_t, N_c and a, i.e.,

$$sgn(b_{\text{crit}}) = sgn\left(\frac{72}{\lambda} - 1\right) \quad (47)$$

All these features are illustrated in Fig. 3. Figure 3 also shows that the function $b_{\text{crit}} = b_{\text{crit}}(a)$ always possesses an

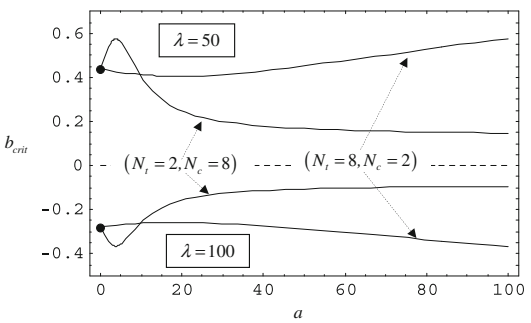

Fig. 3 Shown are the plots of b_{crit} as functions of a in two typical cases with $N_t < N_c$ and $N_t > N_c$, when $\lambda = 50$ (upper half-plane) and $\lambda = 100$ (lower half-plane). The critical values of the buoyancy ratio b are positive when $\lambda < 72$ and negative when $\lambda > 72$, in a full agreement with Eq. 47, no matter whether $N_t > N_c$ or $N_t < N_c$. The *dots* mark the points of coordinates $(a, b_{\text{crit}}) = (0, 72/\lambda - 1)$

absolute extremum (maximum or minimum) at a certain value of a both for $N_t > N_c$ and $N_t < N_c$.

We mention that at the critical value (43) of the buoyancy ratio b, the crossover of the velocity field from the unidirectional to bidirectional structure, qualitatively resembles in all cases the special situation illustrated in Fig. 2, except for the existence of the intersection point (36).

4.4 The pressure gradient α

The explicit expression of the dimensionless pressure gradient α is given by Eq. 26 which involves all the five parameters λ, b, N_t, N_c and a. However, an important physical feature of α is that it does not depend on the mixed convection parameter λ and the buoyancy ratio b independently, but only on their product λb. In Fig. 4 α is plotted as a function of the effective thermophoretic coefficient a for $N_t = 8$, $N_c = 2$ and five different values of λb (assuming tacitly that $\lambda > 0$). One sees that α decreases monotonically with increasing values of a when $\lambda b < 0$, while for $\lambda b = 0$ it takes the constant value -12, in agreement with Eq. 33. For positive values of λb, α increases monotonically with increasing a and, at a certain value a_0 of a it becomes zero, changing then from negative to positive values. This happens at $a_0 = 13.6739$ for $\lambda b = 100$, and at $a_0 = 6.51972$ for $\lambda b = 200$, respectively.

The intersection points of the curves $\alpha(a)$ with the a-axis correspond to the remarkable physical situations where the driving pressure equals the local hydrostatic pressure everywhere. The corresponding flows are always bidirectional. This latter feature is illustrated in Fig. 5 where the two velocity profiles are shown which correspond to the points $(a, \alpha) = (a_0, 0)$ marked by dots in Fig. 4.

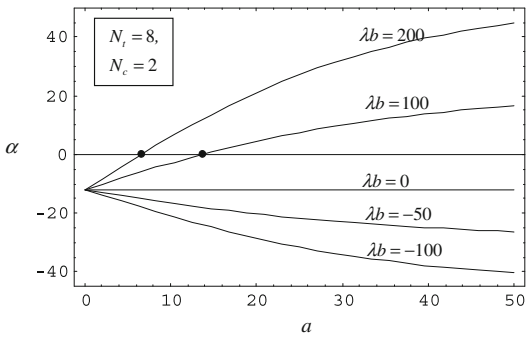

Fig. 4 Plots of the dimensionless pressure gradient α as a function of a for the indicated values of the parameters N_t, N_c and λb. All the curves start at $a = 0$ in the point $\alpha = -12$ in agreement with Eq. 33. The *dots* mark the zeros of α for $\lambda b > 0$

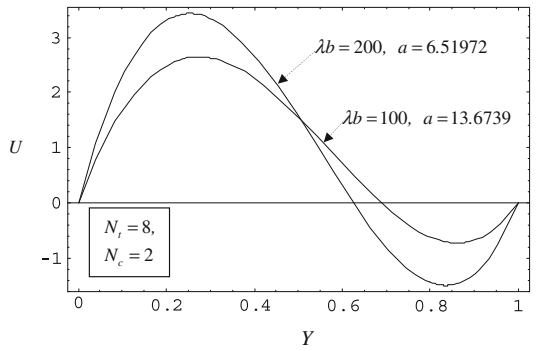

Fig. 5 Shown are the velocity profiles which are associated with the intersection points of the curves $\alpha(a)$ of Fig. 4 with the a-axis. These bidirectional flows correspond to $\alpha = 0$, i.e., to the situations in which the driving pressure equals the local hydrostatic pressure of the gas everywhere in the vertical channel

5 Summary and conclusions

In the present paper the full analytical solution of the title problem investigated recently by Grosan et al. [1] by numerical methods, has been presented and discussed in detail. The motivation for our work was the high complexity of a comprehensive numerical investigation of this problem which, in addition to the unknown pressure gradient α, involves further six dimensionless parameters, N_t, N_c, λ, b, k and Sc.

The key point of the present analytical approach is the use a *first integral* of the concentration equation, instead to keep this equation in its initial second order form (see Eq. 13 of [1]). The first order equation obtained in this way admits a closed form solution for the dimensionless concentration field which depends only on powers of the transformed transverse coordinate $Z = (N_t + 1/2) - Y$. Subsequently, the velocity equation could also be integrated twice with respect to the variable Z directly. The new knowledge gained from the analytical approach can be summarized as follows.

1. The effect of thermophoresis on the concentration and velocity fields does not depend on the thermophoretic coefficient k and the Schmidt number Sc separately, but it is controlled by an *effective thermophoretic coefficient* a, which is the dimensionless group $a = kSc$. Accordingly, the concentration distributions ϕ of the fully developed channel flow associated with different values of k and Sc, but the same value of a, N_t and N_c, are physically equivalent (see Eq. 21). This *principle of equivalent states* is a consequence of the interplay between thermophoresis (driven by temperature gradients) and diffusion (driven by concentration gradients). Owing to this feature, the present problem involves, instead of six, five effective parameters only. These are N_t, N_c, a, λ and b.

2. The Sherwood numbers $Sh_{0,1}$, i.e., the negative concentration gradients at the walls $Y = 0$ and $Y = 1$ of the channel, can be calculated explicitly (see Eq. 28). Their difference, $Sh_1 - Sh_0$, represents the thermophoretic deposition flux of the particles on the cold wall when $N_t > N_c$, and the ablation flux from the same wall when $N_t < N_c$. With respect to the wall conditions, the inequality $N_t > N_c$ corresponds to the situation in which $T_c/T_h > C_c/C_h$ and $N_t < N_c$ to $T_c/T_h < C_c/C_h$, respectively.
3. The concentration ϕ is always a monotonically decreasing function of the transverse coordinate Y when $N_t > N_c$. This property holds also for $N_t < N_c$ when the effective thermophoretic coefficient a is small. However, for sufficiently large values of a (specified by the second condition (32)) the concentration ϕ decreases to a minimum value $\phi_{\min} < -1/2$ reached at some $Y = Y_*$ (see Eqs. 31), and then increases to the wall value $\phi = -1/2$ as $Y \to 1$. These properties of ϕ are illustrated in Fig. 1.
4. The exact velocity solution U given by Eq. 23 involves in general the powers Z, Z^2 and Z^3 and Z^{2-a} of the transformed transverse coordinate $Z = (N_t + 1/2 - Y)$, except for the special values $a = 1$ and $a = 2$ of the effective thermophoretic coefficient where the power Z^{2-a} is missing and, instead, the logarithmic expressions $ZlnZ$ and lnZ occur (see Eqs. 38 and 40). Such intrinsic properties cannot be seen in a numerical approach.
5. The critical value b_{crit} of the buoyancy ratio where the velocity field U changes from a unidirectional to a bidirectional structure can also be calculated exactly (see Eqs. 43–46 and Fig. 2). The sign of b_{crit} is determined by the value of the mixed convection parameter alone, namely $b_{\text{crit}} \geq 0$ when $\lambda \leq 72$ and $b_{\text{crit}} \leq 0$ when $\lambda \geq 72$ (see Eq. 47). There also turns out that the function $b_{\text{crit}} = b_{\text{crit}}(a)$ always possesses an absolute extremum (maximum or minimum) at a certain value of a, both for $N_t > N_c$ and $N_t < N_c$ (see Fig. 3).
6. Surprisingly, the special cases ($N_t = N_c$; $a \neq 0$) and ($N_t \neq N_c$; $a = 0$) with and without thermophoresis, are physically undistinguishable. In both of these cases the respective expressions of the experimentally accessible quantities θ, ϕ, U and α are the same (see Eqs. 30, 35 and 33). In other words, between the thermophoretic effect governed by the parameter a and the temperature and concentration boundary conditions governed by the parameters N_t and N_c, a remarkable compensation effect can occur which renders the above cases with ($a \neq 0$) and without ($a = 0$) thermophoresis equivalent. As we are aware, this compensation effect has not been reported before in the pertinent literature.
7. Similarly to the velocity solution (23), the explicit solution (26) for the dimensionless pressure gradient α also includes all the five effective parameters N_t, N_c, a, λ and b of the problem. However, a physically important property of α is that it does not depend on the mixed convection parameter λ and the buoyancy ratio b separately, but on their product λb only. Thus, when either $\lambda = 0$ or $b = 0$, α renders the same value -12 as in the pure forced convection channel flow (Poiseuille flow). The value $\alpha = -12$ is also obtained in the absence of thermophoresis ($a = 0$) in general, as well as in the two mutually compensating cases ($N_t = N_c$; $a \neq 0$) and ($N_t \neq N_c$; $a = 0$) discussed under Point 6 above. (see also Eq. 33).
8. For $N_t > N_c$, the dimensionless pressure gradient α is a monotonically decreasing or increasing function of the effective thermophoretic coefficient a depending on whether $\lambda b < 0$ or $\lambda b > 0$, respectively (see Fig. 4). For $N_t < N_c$, the converse holds. At a certain value a_0 of a, the increasing pressure gradient becomes zero and changes sign (see Fig. 4). These intersection points of the curves $\alpha(a)$ with the a-axis correspond to the remarkable physical situations where the driving pressure equals the local hydrostatic pressure everywhere in the flow domain of the fully developed regime. The corresponding flows are always bidirectional (see Fig. 5).

References

1. Grosan T, Pop R, Pop I (2009) Thermophoretic deposition of particles in fully developed mixed convection flow in a parallel-plate vertical channel. Heat Mass Transf 45:503–509
2. Selim A, Hossain MA, Rees DAS (2003) The effect of surface mass transfer on mixed convection flow past a heated vertical flat permeable plate with thermophoresis. Int J Therm Sci 42:973–982
3. Postelnicu A (2007) Effects of thermophoresis particle deposition in free convection boundary layer from a horizontal flat plate embedded in a porous medium. Int J Heat Mass Transf 50:2981–2985
4. Chamka A, Pop I (2004) Effect of thermophoresis particle deposition in free convection boundary layer from a vertical flat plate embedded in a porous medium. Int Commun Heat Mass Transf 31:421–430
5. Talbot L, Cheng RK, Schefer AW, Willis DR (1980) Thermophoresis of particles in a heated boundary layer. J Fluid Mech 101:737–758
6. Brock JR (1962) On the theory of thermal forces acting on aerosol particles. J Colloid Sci 17:768–770
7. Hales JM, Schwendiman LC, Horst TW (1972) Aerosol transport in a naturally-convected boundary layer. Int J Heat Mass Transf 15:1837–1849
8. Goren SL (1977) Thermophoresis of aerosol particles in the laminar boundary layer on a flat plate. J Colloid Interface Sci 61:77–85

9. Epstein M, Hauser GM, Henry RE (1985) Thermophoretic deposition of particles in natural convection flow from a vertical plate. ASME J Heat Transf 107:272–276
10. Batchelor GK, Shen C (1985) Thermophoretic deposition in gas flow over cold surfaces. J Colloid Interface Sci 107:21–37
11. Garg VK, Jayaraj S (1988) Thermophoresis of aerosol particles in laminar flow over inclined plates. Int J Heat Mass Transf 31:875–890
12. Garg VK, Jayaraj S (1990) Thermophoretic deposition over a cylinder. Int J Eng Fluid Mech 3:175–196
13. Chein R, Liao W (2005) Thermophoretic effects on nano-particle deposition in channel flow. Heat Mass Transf 42:71–79
14. Wang C-C (2006) Combined effects of inertia and thermophoresis on particle deposition onto a wafer with wavy surface. Int J Heat Mass Transf 49:1395–1402
15. Wang C-C, Chen C-K (2006) Thermophoresis deposition of particles from a boundary layer flow onto a continuously moving wavysurface. Acta Mech 181:139–151
16. Aung W (1972) Fully developed laminar free convection between vertical plates heated asymmetrically. Int J Heat Mass Transf 15:1577–1580